Influence of Tyrosine on the Electronic Circular Dichroism of Helical Peptides

Samita Bhattacharjee,[†] Gergely Tóth,[‡] Sándor Lovas,[‡] and Jonathan D. Hirst*,[†]

School of Chemistry, University of Nottingham, University Park, Nottingham NG7 2RD, U.K., and Department of Biomedical Sciences, School of Medicine, Creighton University, 2500 California Plaza, Omaha, Nebraska 68178

Received: February 28, 2003; In Final Form: May 28, 2003

Studies of short helical peptides can provide insights into amino acid interactions in proteins and their role in protein folding. A common method of estimating helical structure is electronic circular dichroism (CD) in the far ultraviolet. It is known that aromatic side chains such as tyrosine may influence CD in this region, but this residue has desirable fluorescent properties and is nevertheless often incorporated into peptides. To investigate the relationship between the conformation of tyrosine and its contribution to the CD, we have calculated the CD of some short alanine-based helical peptides from first principles based on molecular dynamics simulations. The calculations are complemented by some analysis of static models. These theoretical studies estimate that a tyrosine residue may contribute up to ±5000 deg cm^2 dmol^{-1} to the mean residue ellipticity at 220 nm, with the most typical value being 1000 deg cm^2 dmol^{-1}. If uncorrected, this would lead to an underestimate of the helicity of the peptide of 5−20%. For a tyrosine side chain in the trans rotameric state, there is a discernible relationship between its precise orientation and its contribution to CD at 220 nm. Experiments on tyrosine-containing peptides using CD should be interpreted bearing these findings in mind and, preferably, with an independent approach for probing the conformational states of tyrosine.

Introduction

One of the most successful applications of far-ultraviolet circular dichroism (far-UV CD) spectroscopy—the structural characterization of proteins—depends on its sensitivity to the backbone conformation of proteins. The characteristic CD spectrum of a protein depends on its secondary structure content;[1,2] for example, the spectrum of an α-helix consists of a positive band at 190 nm and two negative bands at 208 and 220 nm,[3] whereas β-sheet proteins have a maximum at 195 nm and a minimum in the region of 210−220 nm. The helix content of a peptide is often determined by the intensity of the negative peak at 220 nm.[4,5] The interpretation of CD spectra, however, is complicated by aromatic side-chain chromophores.[6−8] Their contribution depends on the electronic transitions of the aromatic chromophore, the conformation of the aromatic side chain, the proximity of other aromatic residues, and the structure of the polypeptide chain in which they are located. Studies of several proteins in the far-UV have demonstrated that unusual CD spectra arise from the presence of tyrosine, histidine, tryptophan, and phenylalanine side chains.[6,9] For example, Freskgård et al. have shown this through the experimentally determined CD spectra of carbonic anhydrase and several mutants involving tyrosine.[9] Vuilleumier et al. reported analogous studies of barnase and mutants involving tyrosine and tryptophan.[10]

Electronic CD has been widely used to investigate the propensities of amino acids to form α-helices in short peptides.[1−4] In peptides including aromatic residues, potential artifacts resulting from distortions of the CD spectrum, distinct from any induced conformational changes, are unavoidable. Thus, a theoretical estimate of the influence of the aromatic side chain on CD would allow a more accurate estimate of the helix content of peptides. Recently, there have been significant improvements in the accuracy of calculations of the CD of proteins from first principles[11,12] based on modern quantum mechanical calculations on the amide group combined with a continuum model of solvent effects.[13] Other recent calculations[14,15] are also of comparable accuracy. The quality of the calculations based on the improved quantum chemistry has given us confidence to use them to estimate the influence of aromatic side-chain chromophores on the CD spectra of peptides.[16] As part of a study of aromatic interactions in short helical peptides, the helicity estimated from the intensity at 222 nm was corrected using a first principles calculation of the CD starting from a given set of atomic coordinates.

There have been several theoretical studies of the influence of aromatic groups on the CD of proteins. Cooper and Woody studied tropomyosin,[17] focusing on the effect of conformation on the CD of the interacting helices. They modeled the system as two 21-residue α-helices distorted to a coiled-coil conformation. Strong coupling exciton theory was used to compute the optical properties of the system. Two backbone amide electronic excited states, nπ^* and $\pi\pi^*$, were considered, as well as four excited states for the phenolic side chain, denoted in Platt's notation[18] as L_b, L_a, B_b, and B_a. Extensive calculations of steric interactions between the phenolic rings and between the rings and the α-helix backbone were performed. The rotational strength of the phenolic L_b transition was calculated as a function of position within the heptad repeats and as a function of the side-chain dihedral angles, χ_1 and χ_2. Tryptophan was the focus of a study by Grishina and Woody,[19] who estimated the contribution of the tryptophan B_b transition to the far-UV CD spectra of dihydrofolate reductase, barnase, chymotrypsin, and chymotrypsinogen. Difference spectra were computed for wild-type proteins and mutants, and some agreement with experiment

* Corresponding author. E-mail: jonathan.hirst@nottingham.ac.uk. Fax: +44 115 951 3562.
† University of Nottingham.
‡ Creighton University.

10.1021/jp034517j CCC: $25.00
Published on Web 07/11/2003

was reported. More recently,[20] an improved parameter set for side-chain chromophores was used to compute the CD spectra of bovine pancreatic trypsin inhibitor and various mutants. We use some of those parameters in the current work.

In our study, the effect of the interaction between the aromatic side chain of tyrosine and the helical backbone on the CD spectrum is investigated using molecular dynamics (MD) and CD calculations. Using a set of parameters derived from ab initio calculations and the origin-independent matrix method,[21,22] the calculated CD spectrum is analyzed over the MD trajectory to understand the effect of tyrosine conformation on CD. For each of seven peptides, the relationship between the conformational dynamics and the ab initio-based CD spectrum is investigated from the MD trajectories comprising 10 000 snapshots. CD calculations from first principles offer a number of advantages over simple empirical approaches, which are based on ad hoc definitions of helical conformation. Short peptides are more flexible than proteins and adopt conformations that are quite distinct from typical geometries of native proteins. In contrast to an empirical approach, first principles calculations do not require the explicit assumption that certain sets of conformations contribute uniformly to the CD spectrum and that other conformations contribute nothing. First principles CD calculations are based on the interactions between the electronic transitions of the backbone chromophores and aromatic side chains, allowing one to examine the influence of the tyrosine residue on the measured CD spectrum and to differentiate this influence from its effect on the structure of the peptide.

In our study, static models of alanine-based α-helical peptides with tyrosine side chains are also built to predict the effect of tyrosine on CD. In addition, we examine a model peptide with two tyrosine residues to investigate the effect of side chain−side chain interactions on the CD of peptides. We focus on the calculated intensity at one wavelength of the computed spectra, 220 nm. The intensity at 220 nm is widely used to estimate the helicity of proteins and peptides.[23] The calculations are particularly reliable at 220 nm.[11] To investigate the influence of the tyrosine residue on the CD, we compare calculations of the CD spectra with and without parameters for the electronic transitions associated with tyrosine.

Methods

Static Models of Peptides. Models were constructed for the sequences Ac-Ala_{11}TyrAla$_{10}$-NH_2 and Ac-Ala_{13}TyrAla$_8$-NH_2. A peptide containing two tyrosines, Ac-Ala_5TyrAla$_5$TyrAla-NH_2, was also generated. In these model peptides, the χ_1 dihedral angle has been varied in steps of 10° around the trans and gauche$^+$ conformations to investigate the effect of the tyrosine conformation on CD. No constraints were placed on χ_2. The macromolecular modeling software CHARMM[24] was used to generate the structures. The peptides were modeled with all of the backbone dihedral angles ($\phi = -63°$, $\psi = -41°$) corresponding to average values observed in helices in known protein structures.[25] Lowest-energy conformations were obtained through steepest descents energy minimization within the generalized Born implicit continuum solvent model with the dielectric constant $\epsilon = 80$ for water.[26,27] In the continuum approach, the solvent is modeled by a continuum characterized by a dielectric constant in which there is a cavity that contains the solute. This provides a macroscopic description of the solvent; short-range solute−solvent interactions such as hydrogen bonding are neglected. To generate the desired geometry, a restraining potential on the dihedral angles was used with the force constant of 1000 kcal mol^{-1} rad^{-2}.

TABLE 1: Peptide Sequences

peptide	amino acid sequence
Y0	Ac-AlaAlaAlaAlaAlaAlaGluAlaAlaLysAla-NH_2
Y1	Ac-TyrAlaAlaAlaAlaAlaGluAlaAlaLysAla-NH_2
Y2	Ac-AlaTyrAlaAlaAlaAlaGluAlaAlaLysAla-NH_2
Y3	Ac-AlaAlaTyrAlaAlaAlaGluAlaAlaLysAla-NH_2
Y4	Ac-AlaAlaAlaTyrAlaAlaGluAlaAlaLysAla-NH_2
Y5	Ac-AlaAlaAlaAlaTyrAlaGluAlaAlaLysAla-NH_2
Y6	Ac-AlaAlaAlaAlaAlaTyrAlaGluAlaAlaLysAla-NH_2

Simulations of Alanine-Based Peptides. We have investigated the contribution of the side-chain tyrosine chromophores to CD using MD simulations of the seven peptides in Table 1. These peptides have been previously studied using MD, CD, and NMR.[28] The synthesis, purification, and vibrational CD of these peptides have been described recently.[29] The template peptide, Y0, was mostly composed of alanine and has 12 residues. To increase the solubility of the host peptide in water, glutamic acid was inserted into the inner helix at position 8, and lysine was placed in C-terminal position 11, where it may further stabilize the helical structure of the host peptide because its positively charged side chain can interact with the macrodipole of the α-helix. Tyrosine was substituted for alanine in positions 1−6; these peptides are named Y1, Y2, Y3, Y4, Y5, and Y6, respectively.

The MD calculations were performed previously[28] using the modified GROMOS-87 force field as implemented in the GROMACS 2.0 program package.[30] The starting structures of the helical peptides were created with Sybyl 6.2,[31] and the χ_1 torsion angle of tyrosine was set to 180°. The side chains of Glu and Lys were negatively and positively charged, respectively. All systems were energy minimized using steepest descents until the difference between the total potential energy of the molecular system in two adjacent energy-minimization steps was less than 0.001 kJ mol^{-1}. MD trajectories of 20 ns were generated at constant temperature, 300 K, and constant pressure, 1 atm. The coordinates of the peptide were stored every 2 ps to yield a total of 10 000 sampled conformations for every trajectory. Further details of the MD simulations will be given elsewhere.

The assignment of the helical structure of the peptide in each trajectory was based on patterns of the helical hydrogen bonding using the DSSP program.[32] In DSSP, an ideal hydrogen bond is one where the amide NH bond and the carbonyl CO bond are collinear and the hydrogen bond length is 2.9 Å. Specifically, main-chain i, $i + 4$ hydrogen bonds were counted, with some deviation permitted from the ideal geometry. As we focus on the effect of tyrosine on the CD of helical peptides, a region in a peptide is considered to be helical when it has at least seven contiguous main-chain i, $i + 4$ hydrogen bonds. Throughout this article, these sets of structures will be referred to as contiguous helical structures. Contiguous helices containing tyrosine were also identified in each trajectory. Because we are interested in the effect of the conformational dynamics of tyrosine on the CD spectrum, contiguous helical structures were further classified into trans, gauche$^-$, and gauche$^+$ rotamers on the basis of the tyrosine side-chain χ_1 angle: trans, $\chi_1 = 180 \pm 60°$; gauche$^-$, $\chi_1 = 60 \pm 60°$; and gauche$^+$, $\chi_1 = -60 \pm 60°$. The gauche$^-$ rotamer is rarely observed in helical structures because of an unfavorable steric interation.[33,34]

CD Calculations. A common method of computing the CD spectra of polypepetides is the matrix method[21,22] because the electronic structure of polypeptides is beyond the scope of ab initio calculations. In the matrix method, a polypepetide is viewed as a collection of chromophoric groups. Electronic

excitations within a group are treated explicitly by ab initio quantum mechanical methods, whereas the interaction between these excited states is computed classically on the basis of parametrizations of the ab initio calculations on the individual chromophores. A Hamiltonian matrix is constructed. The diagonal elements of this matrix are the excitation energies of the single chromophores, and the off-diagonal elements describe the interactions between different chromophoric groups. Thus, the matrix method requires parameters that describe the charge distributions associated with the different electronic states of the chromophoric groups of the protein. In this study, these parameters were taken from calculations[13] on *N*-methylacetamide in solution using the complete-active-space self-consistent field method implemented within a self-consistent reaction field.[35] The interaction potentials were evaluated by representing the charge densities with a set of point charges (or monopoles). The point charges are fitted to reproduce the ab initio electrostatic potential arising from the various states,[11] thereby improving the representation of the monomer. These parameters perform at least as well[12] as other available modern parameters, such as those[15] derived from a combination of INDO/S calculations and experimental data.

Diagonalizing the Hamiltonian yields the eigenvalues and eigenvectors of the composite transitions of the protein. The eigenvalues are the energies of the transitions of the polypeptide, and the eigenvectors give the mixing coefficients describing contributions of the excited states of the individual groups to the delocalized excited states of the polypeptide. The rotational strengths corresponding to each excited state of the polypepetide are derived directly from the electronic and magnetic transition dipole moments. In general, each transition from the ground state to one of the excited states may have nonzero rotational strength at its particular transition energy. The CD spectrum is calculated from the sum of all of these rotational strengths. The detailed methodology is given elsewhere.[11,12]

Two peptide transitions are considered: the nπ* transition at 220 nm and the $\pi\pi$* transition at 193 nm. Higher-energy transitions are not considered because they lie outside the region of interest and the reliability of the parameter sets describing them has yet to be fully established. In addition, four $\pi\pi$* transitions due to the tyrosine chromophore are included: L_a at 227 nm, L_b at 278 nm, B_a at 193 nm, and B_b at 192 nm. We use the recent parameter set for tyrosine of Woody and coworkers.[20] Transitions in the peptide CD spectrum are assumed to have a bandwidth of 15.5 nm. The CD spectrum in the range of 100 to 300 nm was computed for each of the 10 000 snapshots.

If the interactions between individual chromophoric groups are assumed to be purely electrostatic in nature, then the off-diagonal elements are computed from the electrostatic interaction between charge densities and have the form

$$V_{i0a;j0b} = \int\int \frac{\rho_{i0a}(\mathbf{r}_i)\,\rho_{j0b}(\mathbf{r}_j)}{4\pi\epsilon_0 r_{i,j}} \mathrm{d}\mathbf{r}_i\,\mathrm{d}\mathbf{r}_j \qquad (1)$$

where ρ_{i0a} and ρ_{j0b} represent the transition electron densities on chromophores i and j for electronic transitions from the electronic ground state to excited states a and b, respectively and $\mathbf{r}_i$ is the position vector of the electron involved in the transition centered on chromophore i. Similarly, $\mathbf{r}_j$ refers to chromophore j, and the separation of the two electrons is $r_{i,j}$. If only nπ* and $\pi\pi$* transitions are considered, then in the simplest case of a diamide the Hamiltonian matrix takes the form

$$H = \begin{pmatrix} E^1_{\mathrm{n}\pi^*} & V^{11}_{\mathrm{n}\pi^*\pi\pi^*} & V^{12}_{\mathrm{n}\pi^*\mathrm{n}\pi^*} & V^{12}_{\mathrm{n}\pi^*\pi\pi^*} \\ V^{11}_{\mathrm{n}\pi^*\pi\pi^*} & E^1_{\pi\pi^*} & V^{21}_{\mathrm{n}\pi^*\pi\pi^*} & V^{12}_{\pi\pi^*\pi\pi^*} \\ V^{12}_{\mathrm{n}\pi^*\mathrm{n}\pi^*} & V^{21}_{\mathrm{n}\pi^*\pi\pi^*} & E^2_{\mathrm{n}\pi^*} & V^{22}_{\mathrm{n}\pi^*\pi\pi^*} \\ V^{12}_{\mathrm{n}\pi^*\pi\pi^*} & V^{12}_{\pi\pi^*\pi\pi^*} & V^{22}_{\mathrm{n}\pi^*\pi\pi^*} & E^2_{\pi\pi^*} \end{pmatrix} \qquad (2)$$

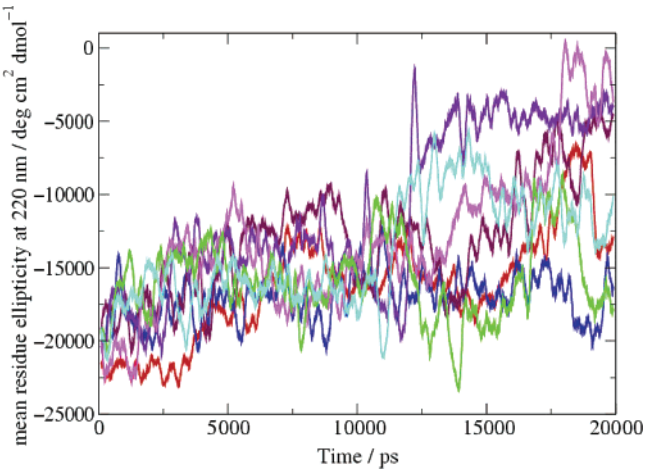

Figure 1. Time evolution from MD simulation of CD intensity at 220 nm of the peptides: Y0 (red), Y1 (blue), Y2 (maroon), Y3 (violet), Y4 (magenta), Y5 (green), Y6 (turquoise). Peptide sequences are given in Table 1.

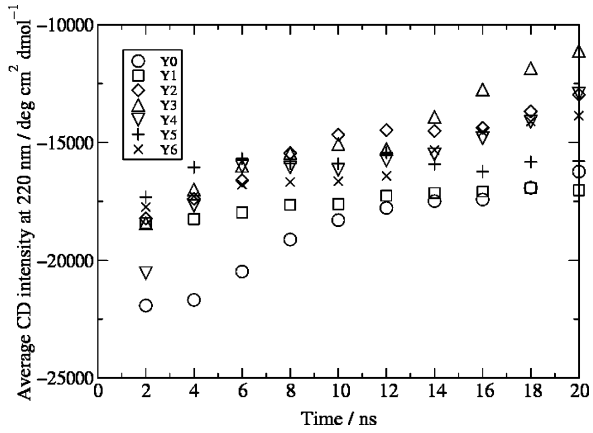

Figure 2. Average value of CD intensity at 220 nm for 2-ns intervals from MD simulation. Peptide sequences are given in Table 1.

The off-diagonal elements give the interactions between the excited states within an individual chromophore and also between the excited states of different chromophores. We have examined these matrix elements in detail because their values reflect the importance of difference interactions in determining the CD spectrum.

Results

The evolution of the calculated CD intensity at 220 nm is shown in Figure 1 for the seven 12-residue peptides. The data in the Figure have been smoothed, using a running average over 100 snapshots, so that the fluctuations in the intensity (which are significantly greater than shown in the Figure) do not obscure the underlying trends. Figure 2 shows the average value of the CD intensity at 220 nm over 2-ns intervals. The Figures suggest that the peptides with a tyrosine residue at the first (Y1) or fifth position (Y5) are most helical over the course of the simulation; the template peptide (Y0), which has no tyrosine, is also quite

TABLE 2: Helical Populations in Simulations of Peptides Y0−Y6 as Defined in Table 1

peptide	no. of helical structures	no. of contiguous helical structures[a]	number of contiguous helical structures with tyrosine in the helix			
			trans	gauche$^+$	gauche$^-$	total
Y0	7737	6847	N/A	N/A	N/A	N/A
Y1	8552	6964	5211	964	0	6175
Y2	6028	5816	923	1509	4	2436
Y3	2791	1463	1426	0	0	1426
Y4	7965	7498	5311	1149	0	6460
Y5	6995	6805	4690	1862	0	6552
Y6	5801	2131	700	1043	0	1743

[a] Conformations with more than one contiguous helix are rare, so the fraction of conformations that contain a contiguous helix may be estimated by dividing the values in this column by 10 000.

helical. The peptide with tyrosine in the sixth position (Y6) is a little less helical. The least helical peptides are those with tyrosine at the second, third, or fourth position (Y2, Y3, and Y4). Several peptides show considerable unfolding in the second half of the trajectory.

The presence of tyrosine changes the conformations populated by the peptides as shown in Table 2. The total number of helices, number of contiguous helices, and number of contiguous helices containing tyrosines within them are calculated on the basis of the i, $i + 4$ backbone interactions using the DSSP program for the trajectories of the seven peptides. Structures are considered to be helical when they possess a minimum of seven i, $i + 4$ hydrogen bonds. Y4 has the highest number of contiguous helices. Y0, Y1, and Y5 have fewer contiguous helices than Y4; Y3 and Y6 have the fewest. A similar trend is observed for helical structures including tyrosine, except for Y2. The trends in helicity based on the DSSP analysis (Table 2) and the CD calculations (Figure 2) generally agree, although peptide Y4 has a lower average intensity at 220 nm than would be anticipated from the high number of helical conformations. For the tyrosine containing helical structures, the rotamer populations of the tyrosine side chain are also given in Table 2. Among all of the peptides, Y1 and Y4 have the highest number of trans conformers, Y5 populates the trans conformation a little less, and Y2, Y3, and Y6 populate the trans conformation the least. Y3 does not have any gauche$^+$ population; the rest of the peptides show similar gauche$^+$ populations. The rotamer populations are in broad accord with those observed in proteins,[34] where in the interior of helices 66% of tyrosine residues adopt the trans conformer and only 1%, the gauche$^-$.

Correlation between CD and Conformation. The tyrosine residue perturbed the CD spectra of the peptides. We have investigated the contribution to the 220-nm ellipticity through the difference between the computed intensity at 220 nm for calculations that include and ignore the tyrosine transitions. Table 3 shows the mean contribution to the intensity at 220 nm computed over all of the snapshots in the trajectories and within each rotameric state (regardless of the helicity of the peptide). A positive contribution indicates that the CD spectrum is less intense than would be anticipated from the backbone structure alone.

The trans and gauche$^+$ rotamers of tyrosine have been examined separately to probe, within rotameric states, whether there are relationships between tyrosine orientation and CD spectra. In the analysis, only contiguous helices containing tyrosine are considered because the less structured conformations would presumably simply add noise to the underlying relationships. The Pearson correlation coefficient, r, between the difference in CD intensity at 220 nm and the χ_1 dihedral angle of the tyrosine is given in Table 4; for the trans rotamer, only

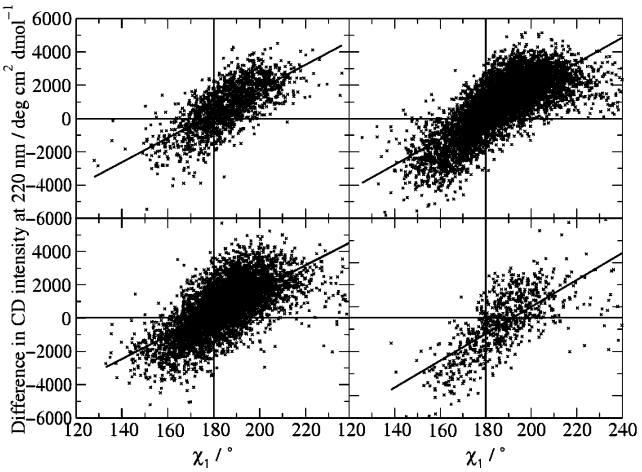

Figure 3. Correlations between χ_1 and difference in the CD intensity at 220 nm for peptides Y3 (top left), Y4 (top right), Y5 (bottom left), and Y6 (bottom right).

TABLE 3: Calculated Tyrosine Contributions to the CD Spectrum at 220 nm for Peptides Y1−Y6 as Defined in Table 1

peptide	population of rotamers (from a sample of 10 000)			mean Tyr contribution to $[\theta]_{220}$/deg cm^2 dmol^{-1}			
	trans	gauche$^+$	gauche$^-$	trans	gauche$^+$	gauche$^-$	total[a]
Y1	8750	1250	0	2039	1472	N/A	1968
Y2	2520	6036	1444	1419	−17	−672	251
Y3	6047	1660	2293	1805	417	−1523	812
Y4	8728	1270	2	2057	1859	−2131	2031
Y5	6652	3345	3	1519	−138	−1996	964
Y6	965	4960	4075	1843	−146	−539	−114

[a] Weighted mean of the values in the preceding three columns.

TABLE 4: Correlation between χ_1 and Changes in the Minimum at around 220 nm for Peptides Y1−Y6 as Defined in Table 1

peptide	Pearson r correlation coefficient			
	correlation of χ_1 with the difference in intensity at 220 nm		correlation of χ_1 with the shift in wavelength of the peak around 220 nm	
	trans	gauche$^+$	trans	gauche$^+$
Y1	0.32	−0.32	−0.17	0.27
Y2	0.37	−0.12	−0.23	0.25
Y3	0.71	N/A	−0.33	0.28
Y4	0.74	−0.29	−0.54	0.27
Y5	0.65	0.12	−0.43	0.12
Y6	0.69	−0.11	−0.42	0.22

χ_1 angles in the range of $180 \pm 60°$ are considered, and for the gauche$^+$ rotamers, only χ_1 angles of $-60 \pm 60°$ are considered. Y1 and Y2 exhibit little correlation in the trans conformations, whereas Y3, Y4, Y5, and Y6 show stronger correlations, with r varying between 0.65 and 0.74. There is no correlation between the difference in the CD intensity at 220 nm and χ_1 when the tyrosine side chain is in the gauche$^+$ conformation. Figure 3 shows the relationship between χ_1 and the difference in intensity at 220 nm for peptides Y3, Y4, Y5, and Y6, which gave the highest correlation coefficients. The correlation between the shift in the precise location of the minimum around 220 nm and χ_1 (given in Table 4) varies between −0.17 and −0.54 in trans conformations and between 0.12 and 0.28 in gauche$^+$ conformations. This is not sufficiently high for any trend to be apparent other than a general tendency for the minimum to shift to longer wavelengths.

TABLE 5: Important Interaction Matrix Elements between Side-Chain and Backbone Transitions for the trans Rotamer of Tyr[a]

peptide		Y1	Y2	Y3	Y4	Y5	Y6
Interaction	Location of Backbone Chromophore Relative to Tyr at Position *i*	Interaction Matrix Element/cm^{-1}					
nπ^*−B_b	*i*	222	231	238	239	240	238
$\pi\pi^*$−L_a	*i* − 1	415	409	422	425	423	424
$\pi\pi^*$−B_a	*i* − 4	N/A	N/A	N/A	207	214	211
	i − 3	N/A	N/A		272	296	285
	i	564	534	561	574	593	565
	i + 1		257				
	i + 3	348	215		214		203
$\pi\pi^*$−B_b	*i* − 4	N/A	N/A	N/A	307	283	304
	i − 3	N/A	N/A	431	457	433	437
	i − 1	769	772	797	805	799	802
	i	370	285	270	244	256	260
	i + 3	222					

[a] N/A indicates that the interaction does not exist at all because of the location of Tyr in the peptide sequence; an empty entry denotes that the value is less than 200 cm^{-1}.

To investigate the correlation (or lack thereof) between the difference in CD intensity at 220 nm and the conformations of tyrosine for peptides Y1 and Y2, the elements of the *V* matrix (described in eq 1) arising from interactions between the L_a, L_b, B_a, and B_b transitions of tyrosine and the nπ^* and $\pi\pi^*$ transition states of the backbone chromophores have been examined. The *V* matrix elements reflect the extent of coupling between electronic transitions. Values greater than 200 cm^{-1} tend to lead to discernible differences in the calculated CD spectrum. Thus, the *V* matrix can provide some insight into which conformations and therefore which interactions are significant and persistent over the course of the simulations.

The root-mean-square values of the *V* matrix elements (computed over the contiguous helical structures) between tyrosine and the peptide groups at positions ($i-4$, $i-3$, $i-2$, $i-1$, i, $i+1$, $i+2$, $i+3$, $i+4$) were computed. Table 5 indicates, for peptides Y1 to Y6 with tyrosine in the trans conformation, the elements of the *V* matrix greater than or equal to 200 cm^{-1}; Table 6 shows the analogous data for tyrosine in the gauche$^+$ conformation. (For peptide Y3, no gauche$^+$ rotamers were observed.) Interactions involving the amide nπ^* transition are much weaker than those of the amide $\pi\pi^*$ transition because the nπ^* transition is only weakly allowed and has an electric transition dipole moment that is 2 orders of magnitude smaller than that of the $\pi\pi^*$ transition. Tables 5 and 6 show that for the Y3, Y4, Y5, and Y6 peptides the (i, $i-4$), (i, $i-3$), (i, $i-2$), and (i, $i-1$) interactions are more significant than the (i, $i+4$), (i, $i+3$), (i, $i+2$), and (i, $i+1$) interactions; the possibility of (i, $i-4$), (i, $i-3$), and (i, $i-2$) contributions does not exist for peptides Y1 and Y2. Specifically, the (i, $i-3$) interactions are most important for the Y3, Y4, Y5, and Y6 peptides.

Static Models of Peptides. Static models of peptides Ac-$Ala_{11}TyrAla_{10}$-NH_2 and Ac-$Ala_{13}TyrAla_8$-NH_2 were considered. The difference in the CD intensity at 220 nm due to the variation of the χ_1 angle of tyrosine for both peptides is given in Figure 4. These results show a trend similar to that observed in the MD simulations. Tyrosine transitions can change the mean residue ellipticity at 220 nm by up to 2000 deg cm^2 dmol^{-1} in either a positive or negative direction. We have examined the *V* matrix elements for both peptides by looking at the same interactions as in peptides Y1−Y6. A similar trend is observed.

TABLE 6: Important Interaction Matrix Elements between Side-Chain and Backbone Transitions for the Gauche$^+$ Rotamer of Tyr[a]

peptide		Y1	Y2	Y4	Y5	Y6
Interaction	Location of Backbone Chromophore Relative to Tyr at Position *i*	Interaction Matrix Element/cm^{-1}				
$\pi\pi^*$−L_a	*i* − 1	573	598	604	600	591
$\pi\pi^*$−B_a	*i* − 4	N/A	N/A	407	456	507
	i − 3	N/A	N/A	275	202	200
	i − 2	N/A	559	251		
	i − 1	396	407	360	252	268
	i	321	343	350	319	339
$\pi\pi^*$−B_b	*i* − 4	N/A	N/A	334	497	525
	i − 3	N/A	N/A	537	472	464
	i − 2	N/A	269			
	i − 1	1074	1114	1194	1151	1159
	i	315	220	243	614	254
	i + 2	206				

[a] N/A indicates that the interaction does not exist at all because of the location of Tyr in the peptide sequence; an empty entry denotes that the value is less than 200 cm^{-1}.

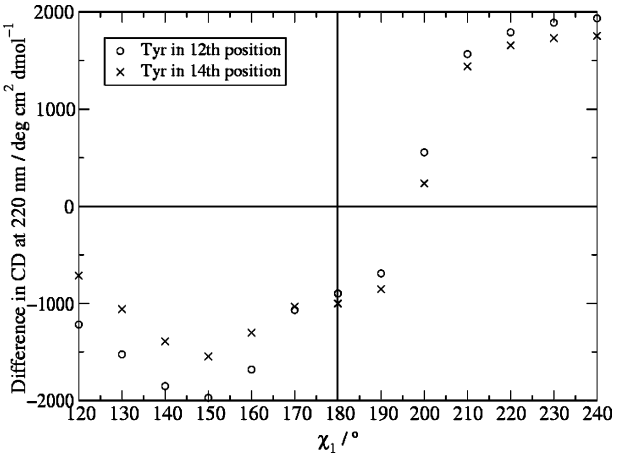

Figure 4. Difference in the CD intensity at 220 nm due to the variation of the tyrosine χ_1 computed from energy minimizations of peptides Ac-$Ala_{11}TyrAla_{10}$-NH_2 and Ac-$Ala_{13}TyrAla_8$-NH_2.

TABLE 7: Mean Interactions between Tyrosine and Backbone Transitions in the Static Model Peptides Ac-$Ala_{11}TyrAla_{10}$-NH_2 and Ac-$Ala_{13}TyrAla_8$-NH_2

location, *j*, of backbone relative to Tyr in the (i, $i+j$) interaction	−5	−4	−3	−2	−1	0	+1	+2	+3
Backbone−Tyr Transitions	Interaction Matrix Element/cm^{-1}								
nπ^*−L_a	17	13	4	3	10	2	2	1	2
nπ^*−L_b	35	36	3	6	115	16	2	3	1
nπ^*−B_a	71	56	21	11	59	13	10	8	11
nπ^*−B_b	96	105	9	14	180	44	5	7	3
$\pi\pi^*$−L_a	97	296	166	39	560	139	19	79	55
$\pi\pi^*$−L_b	44	155	111	64	32	87	36	16	28
$\pi\pi^*$−B_a	168	628	474	282	186	405	157	75	126
$\pi\pi^*$−B_b	240	794	367	92	1103	154	30	181	133

The interaction matrix elements between the transition of the tyrosine side chain at position *i* and the transitions of the backbone chromophores at positions ($i-5$, $i-4$, $i-3$, $i-2$, $i-1$, i, $i+1$, $i+2$, $i+3$) are given in Table 7. The interactions (i, $i+1$), (i, $i+2$), and (i, $i+3$) do not significantly influence the CD spectrum at 220 nm.

The differences in the CD intensity at 220 nm due to the tyrosine residues for various conformations of the two tyrosines in the peptide Ac-$Ala_5TyrAla_5TyrAla$-NH_2 are given in Table

TABLE 8: Contribution of Tyrosines to the CD of Ac-Ala$_5$TyrAla$_5$TyrAla-NH$_2$

side-chain conformation (based on fixing χ_1)		calculated intensity at 220 nm/deg cm^2 dmol^{-1}		
tyrosine 1	tyrosine 2	difference	without tyrosine transitions	with tyrosine transitions
trans	trans	1824	−26 088	−24 263
trans	gauche$^+$	1641	−25 663	−24 022
trans	gauche$^-$	841	−25 828	−24 987
gauche$^+$	trans	1297	−25 063	−23 766
gauche$^-$	trans	926	−26 408	−25 482
gauche$^+$	gauche$^+$	1356	−25 142	−23 786
gauche$^+$	gauche$^-$	342	−25 292	−24 950
gauche$^-$	gauche$^+$	1987	−26 270	−24 283
gauche$^-$	gauche$^-$	523	−25 987	−25 464

8. We inspected the *V* matrix elements for this peptide. The backbone−tyrosine interactions were of similar magnitude and showed the same trend as the peptides with a single tyrosine; namely, the (i, $i + 1$), (i, $i + 2$), (i, $i + 3$), and (i, $i + 4$) interactions do not influence the intensity at 220 nm. The interactions between transitions on the two tyrosine side-chain chromophores were almost always less than 200 cm^{-1}.

Discussion

Side-chain chromophores contribute to the CD of peptides and proteins in the far-UV. We have focused on the contribution of tyrosine to helical peptides, systems with only one or two side chains and a single element of secondary structure, which in these respects are more straightforward than proteins. Brahms and Brahms[36] have proposed a simple correction for side-chain contributions to be applied to the analysis of far-UV CD to estimate protein secondary structure content, and the inclusion of side-chain chromophores in first principles calculations of the CD of proteins is clearly desirable. Some calculations of this type[15] have suggested a modest improvement in the accuracy of the calculated spectra upon the inclusion of side chains; other work[12] has not observed any systematic improvement, and more remains to be done in this area.

Contributions from aromatic side chains in the region of 190−200 nm are anticipated to be significant and larger than at 220 nm. However, 220 nm is the wavelength used to estimate helical content experimentally and is also where our calculations are most reliable. Thus, we have not explored aromatic contributions to the CD spectra at wavelengths other than 220 nm. Another region of interest is the near-UV, where transitions in aromatic side chains give rise to distinctive bands, albeit of lower intensity than in the far-UV. The scope of our study, however, has been the influence on experimental estimates of helical content, especially in peptides.

We have found a correlation between the contribution of tyrosine to CD at 220 nm and the precise conformation of trans rotamers, but this correlation is not evident for tyrosine at the N terminus of the peptide. To understand this, we have investigated the *V* interaction matrix between the electronic states of the backbone and tyrosine. This showed that the (i, $i - 4$), (i, $i - 3$), (i, $i - 2$), and (i, $i - 1$) interactions are larger than the other interactions. Such interactions do not exist in peptides where tyrosine is at the N terminus. Calculations on static models of peptides with tyrosine in the interior of the helix show the same trend as in the simulated structures. Hence, first principles CD calculations on model structures can be used to estimate the effect of side chains on the CD of peptides.

Conformational dynamics are an important aspect of proteins, and peptides exhibit even greater flexibility. The influence of conformational variability on CD spectra has been previously investigated in a number of systems, including a cyclic dipeptide,[37] β-peptides,[38] and proteins.[39] Here, we have used MD simulations to generate a set of typical helical conformations for the peptides in solution. It may be that the conformational space of the peptides has not been sampled sufficiently to represent the experimental ensemble of structures fully, but this was not necessary for our study, in which we simply needed a set of structures spanning a range of typical conformations. The forms of the dynamic models in Figure 3 and the static models in Figure 4 are similar, indicating in both cases the underlying form of the influence of χ_1 on the contribution to CD at 220 nm and, in the case of Figure 3, showing the range of variation. Temperature-dependent CD measurements of the peptides and comparison with theory would be of interest, although sampling the greater conformational flexibility of the peptides at higher temperature would be a challenging problem for MD simulations.

We have investigated the effect of side-chain tyrosine on the spectral intensity of CD at 220 nm on the basis of MD simulations of seven alanine-based peptides. These calculations show that the tyrosine transitions can change the mean residue ellipticity at 220 nm from −5000 deg cm^2 dmol^{-1} to 5000 deg cm^2 dmol^{-1}. If experimental evidence (such as NOE data) were available and indicated a particular value of χ_1 in the range of $180 \pm 60°$, then the results in Figure 4 could be used to provide a more precise correction to the mean residue ellipticity at 220 nm. More generally, for most conformations, the presence of tyrosine leads to a positive contribution to the intensity of about 1000 deg cm^2 dmol^{-1} at 220 nm. These theoretical results are in line with, although lower than, experimental estimates[8] and complement previous work on the effect of aromatic side chains on estimates of helix propensities.[7,16,20] The helicity derived from the intensity of CD at 220 nm for tyrosine-containing peptides will tend to underestimate the helical content of the peptide by between 5 and 20%.

Acknowledgment. We are grateful for financial support from BBSRC (42/B15240), NIH-BRIN (1 P20 RR16469-01), and NSF-EPScOR (EPS-0091900) grants. We thank Dr. Andrew Doig (UMIST, U.K.) for stimulating discussions.

References and Notes

(1) Nakanishi, K.; Berova, N.; Woody, R. W. *Circular Dichroism: Principles and Applications*; VCH Publishers: New York, 1994.
(2) Fasman, G. D. *Circular Dichroism and the Conformational Analysis of Biomolecules*; Plenum Press: New York, 1996.
(3) Holzwarth, G.; Doty, P. *J. Am. Chem. Soc.* **1965**, *87*, 218.
(4) Scholtz, J. M.; Baldwin, R. L. *Annu. Rev. Biophys. Biomol. Struct.* **1992**, *21*, 95.
(5) Marqusee, S.; Baldwin, R. L. *Proc. Natl. Acad. Sci. U.S.A.* **1987**, *84*, 8898.
(6) Woody, R. W. *Biopolymers* **1978**, *17*, 1451.
(7) Manning, M. C.; Woody, R. W. *Biochemistry* **1989**, *28*, 8609.
(8) Chakrabartty, A.; Kortemme, T.; Padmanabhan, S.; Baldwin, R. L. *Biochemistry* **1993**, *32*, 5560.
(9) Freskgård, P. O.; Martensson, L. G.; Jonasson, P.; Jonsson, B. H.; Carlsson, U. *Biochemistry* **1994**, *33*, 14281.
(10) Vuilleumier, S.; Sancho, J.; Loawenthal, R.; Fersht, A. R. *Biochemistry* **1993**, *32*, 10303.
(11) Besley, N. A.; Hirst, J. D. *J. Am. Chem. Soc.* **1999**, *121*, 9636.
(12) Hirst, J. D.; Besley, N. A. *J. Chem. Phys.* **1999**, *111*, 2846.
(13) Besley, N. A.; Hirst, J. D. *J. Phys. Chem. A* **1998**, *102*, 10791.
(14) Bode, K. A.; Applequist, J. *J. Am. Chem. Soc.* **1998**, *120*, 10938.
(15) Woody, R. W.; Sreerama, N. *J. Chem. Phys.* **1999**, *111*, 2844.
(16) Andrew, C. D.; Bhattacharjee, S.; Kokkoni, N.; Hirst, J. D.; Jones, G. R.; Doig, A. J. *J. Am. Chem. Soc.* **2002**, *124*, 12706.
(17) Cooper, T. M.; Woody, R. W. *Biopolymers* **1990**, *30*, 657.
(18) Platt, J. R. *J. Chem. Phys.* **1949**, *17*, 484.
(19) Grishina, I. B.; Woody, R. W. *Faraday Discuss.* **1994**, *99*, 245.
(20) Sreerama, N.; Manning, M. C.; Powers, M. E.; Zhang, J.-X.; Goldenberg, D. P.; Woody, R. W. *Biochemistry* **1999**, *38*, 10814.

(21) Bayley, P. M.; Nielsen, E. B.; Schellman, J. A. *J. Phys. Chem.* **1969**, *73*, 228.
(22) Goux, W. J.; Hooker, T. M., Jr. *J. Am. Chem. Soc.* **1980**, *102*, 7080.
(23) Yang, J. T.; Wu, C. C.-S.; Martinez, H. M. *Methods Enzymol.* **1986**, *130*, 208.
(24) Brooks, B. R.; Bruccoleri, R. E.; Olafson, B. D.; States, D. J.; Swaminathan, S.; Karplus, M. *J. Comput. Chem.* **1983**, *4*, 187.
(25) Barlow, D. J.; Thornton, J. M. *J. Mol. Biol.* **1988**, *201*, 601.
(26) Still, W. C.; Tempczyk, A. L.; Hawley, R. C.; Hendrickson, T. *J. Am. Chem. Soc.* **1990**, *112*, 6127.
(27) Dominy, B. N.; Brooks, C. L., III. *J. Phys. Chem. B* **1999**, *103*, 3765.
(28) Tóth, G.; Kover, K. E.; Hirst, J. D.; Murphy, R. F.; Lovas, S. In *Peptides: The Wave of the Future*; Lebl, M., Houghten, R. A., Eds.; American Peptide Society: San Diego, CA, 2001; pp 303−305.
(29) Borics, A.; Murphy, R. F.; Lovas, S. *Biopolymers* **2002**, *72*, 21.
(30) Berendsen, H. J. C.; van der Spoel, D.; van Drunen, R. *Comput. Phys. Commun.* **1995**, *91*, 43.
(31) *Sybyl Users Manual*; Tripos Inc.: St. Louis, MO, 1996.
(32) Kabsch, W.; Sander, C. *Biopolymers* **1983**, *22*, 2577.
(33) McGregor, M. J.; Islam, S. A.; Sternberg, M. J. E. *J. Mol. Biol.* **1987**, *198*, 295.
(34) Penel, S.; Hughes, E.; Doig, A. J. *J. Mol. Biol.* **1999**, *287*, 127.
(35) Serrano-Andres, L.; Fülscher, M. P.; Karlström, G. *Int. J. Quantum Chem.* **1997**, *65*, 167.
(36) Brahms, S.; Brahms, J. *J. Mol. Biol.* **1980**, *138*, 149.
(37) Fleischhauer, J.; Grötzinger, J.; Kramer, B.; Krüger, P.; Wollmer, A.; Woody, R. W.; Zobel, E. *Biophys. Chem.* **1994**, *49*, 141.
(38) Glätti, A.; Daura, X.; Seebach, D.; van Gunsteren, W. F. *J. Am. Chem. Soc.* **2002**, *124*, 12972.
(39) Hirst, J. D.; Bhattacharjee, S.; Onufriev, A. V. *Faraday Discuss.* **2003**, *122*, 253.